

Article

The Effectiveness of Dental Protection and the Material Arrangement in Custom-Made Mouthguards

Ana Messias ^{1,2,*} , Inês J. Gomes ¹, Paulo N. B. Reis ¹ , Ana M. Amaro ¹  and Maria A. Neto ¹ 

¹ Center for Mechanical Engineering, Materials and Processes (CEMMPRE), Department of Mechanical Engineering, University of Coimbra, 3030-788 Coimbra, Portugal; ines.gomes12@hotmail.com (I.J.G.); paulo.reis@dem.uc.pt (P.N.B.R.); ana.amaro@dem.uc.pt (A.M.A.); augusta.neto@dem.uc.pt (M.A.N.)

² Center for Mechanical Engineering, Materials and Processes (CEMMPRE), Department of Dentistry, University of Coimbra, 3030-788 Coimbra, Portugal

* Correspondence: ana.messias@uc.pt; Tel.: +351-239790700

Featured Application: The findings of this work might be used in the design of mouthguards.

Abstract: Experimental research studies have shown that wearing a mouthguard (MG) is an effective way to prevent tooth or maxillofacial trauma. However, there is a lack of scientific information regarding how the material arrangement within the mouthguard can modify its mechanical response during an impact. Hence, this study aimed to evaluate the influence of material arrangement within custom-made mouthguards on stress transmitted to anterior teeth, bone, and soft tissue after impact. Four 3D finite element models of a human maxilla were reconstructed based on the CBCT of a young patient and analyzed according to the presence or absence of a mouthguard and the type of material arrangement within those with a mouthguard: model NMG with no mouthguard; model CMG representing the conventional arrangement with a single 4 mm-thick ethylene-vinyl acetate (EVA) foil; model FMG presenting layer arrangement with two 1 mm-thick foils of EVA in the outer shell and one 2 mm-thick foil of EVA foam in the core; model HMG presenting a 1 mm-thick compact inner and outer shell of EVA and a 2 mm wide air-filled zone in the core. Linear quasi-static analysis and frontal load were used to simulate an impact with an energy of 4.4 J. Isotropic linear elastic properties were assumed for the bone and teeth but not for the mouthguard protection and oral soft tissues. The results were evaluated and compared in terms of displacement, stretches, and stresses. All the mouthguards analyzed reduced the risk of injury to teeth and bone, reducing the displacement and stress of these structures. However, the implementation of a honeycomb structured layer allowed more significant displacement and deformation of the mouthguard's external layer, thus promoting higher protection of the anatomic structures, namely the root dentin and the bone tissue. Nevertheless, the results also indicate that improving the mouthguard flexibility might increase the soft tissue injuries.

Keywords: custom mouthguards; material arrangement; finite element analysis



Citation: Messias, A.; Gomes, I.J.; Reis, P.N.B.; Amaro, A.M.; Neto, M.A. The Effectiveness of Dental Protection and the Material Arrangement in Custom-Made Mouthguards. *Appl. Sci.* **2021**, *11*, 9363. <https://doi.org/10.3390/app11209363>

Academic Editor: Gianrico Spagnuolo

Received: 9 September 2021

Accepted: 6 October 2021

Published: 9 October 2021

Publisher's Note: MDPI stays neutral with regard to jurisdictional claims in published maps and institutional affiliations.



Copyright: © 2021 by the authors. Licensee MDPI, Basel, Switzerland. This article is an open access article distributed under the terms and conditions of the Creative Commons Attribution (CC BY) license (<https://creativecommons.org/licenses/by/4.0/>).

1. Introduction

The oral health condition of an individual is a determining factor in their health and consequently in their quality of life. Although physical activity is one factor contributing to an individual's health, it is also true that collision or contact sports, and some recreational activities, can expose individuals to harmful impacts in the orofacial region, with the associated risk of injury [1–3]. Reports show that the incidence and prevalence of orofacial lesions tend to increase [4,5], and the majority of those involve the anterior teeth [6].

Meanwhile, significant experimental research studies have shown that wearing a mouthguard (MG) effectively prevents tooth or maxillofacial trauma [7–9]. Finite element models with three-dimensional [8–11] and bidimensional [6,12] analyses have also emphasized the benefits of wearing mouthguards. Hence, the number and type of mouthguards

available nowadays is considerable, especially when compared to those available ten years ago. Moreover, the attributes of mouthguards are not easy to identify because they are influenced not only by the impact absorption ability of the material but also by the occlusal relationship and the conformability of the mouthguards' construction [7]. Nevertheless, the most popular material used for mouthguard production is a low-stiffness 28% ethylene vinyl acetate (EVA) [10], mainly due to its shock-absorbing capabilities and high flexibility. Both characteristics allow relatively high deformation under loads, increasing contact area and time and decreasing the magnitude of peak efforts [4]. The mouthguard thickness is also a parameter design that has been well studied [11–13], and experimental and numerical studies seem to agree in a thickness between 3 and 4 mm. Still, in terms of energy absorption and transmission of forces, 4 mm seems to be the ideal thickness. The material arrangement within the mouthguard design has gained attention from some researchers [14–16].

Regarding this design variable, the experimental works of Westerman et al. [14] and Takeda et al. [15] indicate that the inclusion of one air layer in the mouthguard material improves the characteristic impact of mouthguards. At the same time, the numerical study of Tribst et al. [16] reported some behavior differences. The authors reported that the material's elastic modulus inside the MG influenced the stress distribution on the buccal surface of enamel. However, it did not affect the bone tissue stress, periodontal ligament strain, or root dentin tissue stress. Nevertheless, the numerical study was performed using bidimensional simplifications, namely the plane stress condition, contributing to some differences between the numerical and experimental behaviors [17]. Hence, the numerical models developed in this study use tridimensional constitutive relations, i.e., constitutive equations without any simplification, to verify if this assumption might be a factor contributing to those differences.

The main purpose of this study was to evaluate, through the finite element method, the influence of the material arrangement in a custom-made mouthguard on the stress level of intraoral structures during an impact. The material arrangement included one mouthguard with a layer of soft material, in this case, EVA foam [1], another one considered a space layer between two layers of EVA, and a third model assumed that the mouthguard was produced with a compact EVA layer.

2. Materials and Methods

2.1. Geometrical and Numerical Models

Four 3D finite element models of a human maxilla were constructed based on the CBCT reconstruction of the patient. The selected patient showed no signs of relevant systemic or oral diseases, including severe periodontal disease, and presented normal dentition in the maxilla and mandible. The four finite element models are identified as: No Mouth Protection (NMP); Compact EVA Mouthguard (CMG); Foam EVA Mouthguard (FMG); Hollow EVA Mouthguard (HMG). Figure 1 shows two of the three mouthguard protections and Table 1 presents the main differences between them, namely the material used as well as the total thickness of each layer.

Table 1. Description of the three mouthguard protections, namely, thickness and material.

| Mouthguard Protection | Layer Thickness (mm) | Layer Material |
|-----------------------|----------------------|------------------------|
| Compact Eva (CMG) | 4 | EVA |
| Foam Eva (FMG) | 1/2/1 | EVA/EVA Foam/EVA |
| Hollow Eva (HMG) | 1/2/1 | EVA/hollow (space)/EVA |

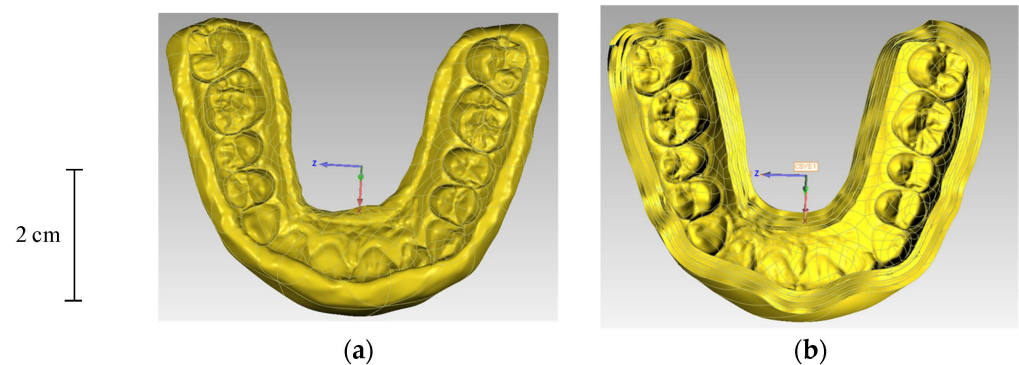


Figure 1. Geometrical model of two mouthguard protections: (a) Compact EVA Mouthguard (CMG); (b) Foam EVA Mouthguard (FMG).

The 3D geometries of the compact and trabecular bones of the maxilla were created by the conversion of the CBCT scan raw medical data into 3D models and, subsequently, were converted to a CAD file by reverse engineering methods [18]. Nevertheless, they were kept undistinguished. The selection of a different threshold for grey values allowed teeth segmentation to be separated from the maxillary bone, but periodontal ligaments were not modeled. The 3D geometrical model of the soft tissue was obtained from the scanning of the external surfaces of the patient maxilla, using an iEOS[®] X5 laboratory scanner (Sirona Dental Systems, Inc.: Erlangen, Germany). The 3D models of the mouthguard protections were created and processed using Geomagic Studio (Geomagic Studio 2013.0.1, Geomagic Inc.: Raleigh, NC, USA) and were posteriorly assembled with the maxillary bone and teeth. After the assembly of all components of the models, the solid bodies were exported in the format of single Parasolid binary files.

All four models were imported into the ADINA system for linear and nonlinear finite element analysis (ADINA AUI version 9.3.1, ADINA R&D Inc.: Watertown, MA, USA). The numerical model of contacts among components was assured using two different contact modeling techniques: the glue mesh option, i.e., assuming that surfaces in contact are perfectly bonded together; the constraint function using Lagrange multipliers, assuring the possibility of relative motion between the contact surfaces. Glue contact was used to bond the outer surfaces of bone and the soft tissue inner surface as well as between maxilla bone and teeth. Relative motion was allowed between the three following contact pairs: soft-tissue/teeth, soft-tissue/mouthguard, and mouthguard/teeth.

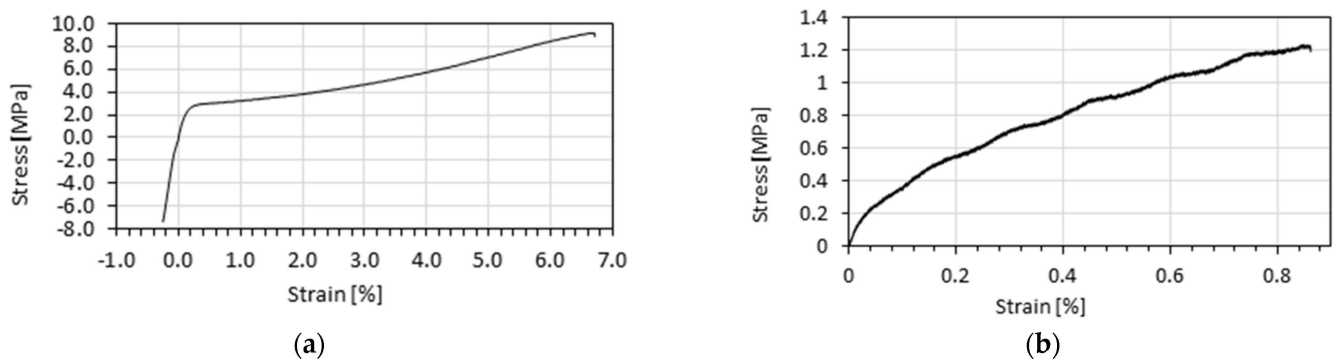
Assignment of the mesh density to the solid bodies of each component was made by promoting equally spaced subdivisions of the volume bodies using the desired element edge length [17]. In some cases, the subdivision of specific faces was recalculated with smaller sizes to promote a more refined mesh in areas requiring higher precision. Table 2 presents the mesh density attributed to each body and the refinement areas. The Delaunay free-form meshing algorithm assured the domains discretization, generating 8-node hexahedral elements. The 8-node elements included a mixed interpolation formulation (displacement and pressure-based) for the almost incompressible materials, i.e., displacements and pressure are interpolated. In addition, the 8-node elements included the incompatible modes features in the domains where the material was not incompressible; the addition of the incompatible modes increases the flexibility of the element, especially in bending solicitation.

Table 2. Description of the length of element edge attributed to each body and the refinement areas.

| Body | Length (mm) | Refinement Zone (mm) |
|-----------------------|-------------|------------------------|
| Bone | 1 | Alveolus region (0.25) |
| Teeth | 0.5 | Root length (0.25) |
| Soft tissue | 0.5 | - |
| Mouthguard Protection | 1 | Crown region (0.5)- |

2.2. Materials. Loadings and Boundary Conditions

This study assumed isotropic linear elastic properties for the bone and teeth but not for the mouthguard protection and the oral soft tissue. The oral mucosa was modelled considering nonlinear hyperelastic properties and the procedure described by Messias et al. [18], while EVA and EVA foam were modelled using the stress-strain curves presented in Figure 2 [1]. The mechanical properties of the materials, displaying a linear force-displacement relationship as implied in Hooke's law, are shown in Table 3.

**Figure 2.** Stress-strain curves of materials used to model mouthguard protection: (a) EVA; (b) EVA Foam.**Table 3.** Mechanical properties of the isotropic linear elastic materials.

| Material | Young's Modulus (GPa) | Poisson' Ratio |
|----------------|-----------------------|----------------|
| Bone | 13.7 [19–22] | 0.30 |
| Teeth (dentin) | 13.0 [23] | 0.37 |

Boundary conditions were applied to the posterior region of the maxilla, as shown in Figure 3a, and all three nodal degrees of freedom were fixed in the areas identified with the letter B. A total force, corresponding to the impact of a hockey ball or roller skates with a mass of 0.155 Kg and with an acceleration of $9.8 \text{ m}\cdot\text{s}^{-2}$, was the main solicitation used in all numerical models. The load was applied over faces/surfaces as a homogeneously distributed pressure in the normal direction, as shown in Figure 3b–d. The two faces or surfaces of the different mouthguards or the two central incisors were loaded to ensure these loading conditions.

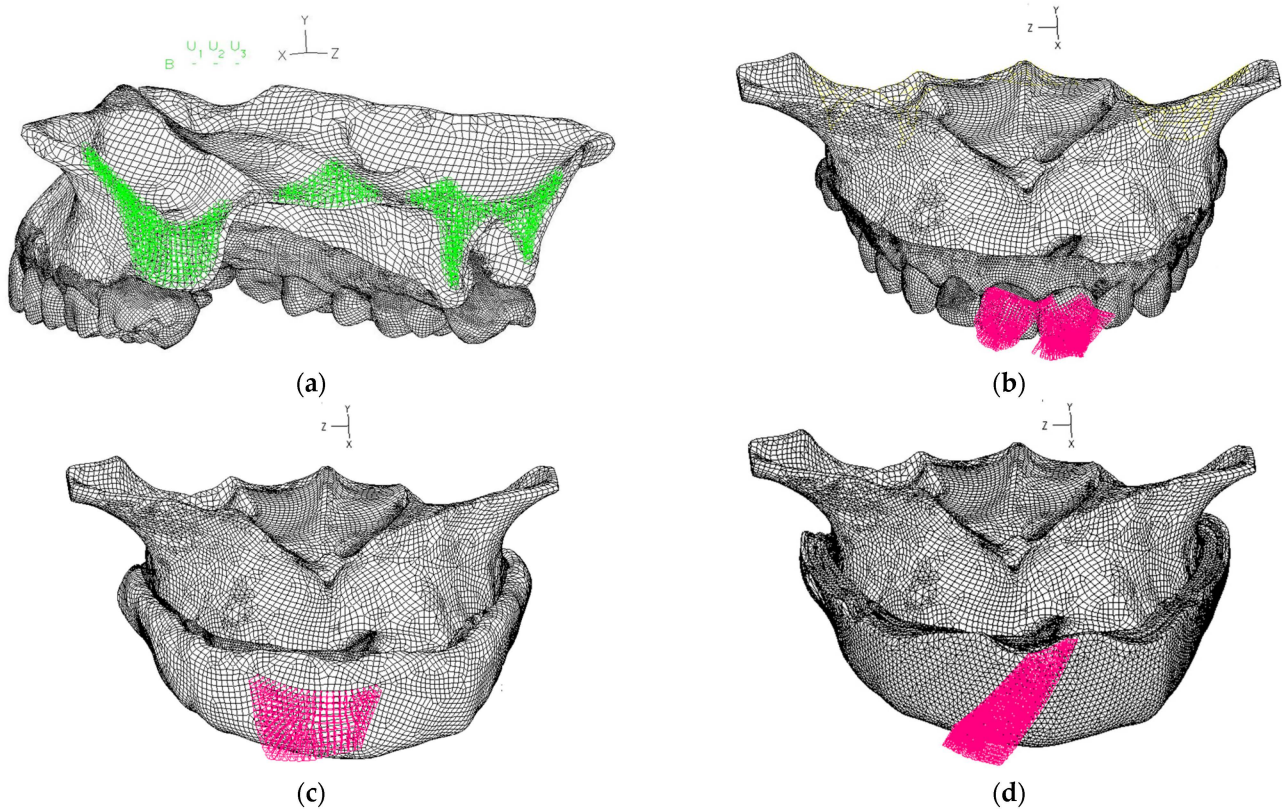


Figure 3. Representation of numerical conditions used within all models: (a) boundary conditions applied on the posterior region of the maxilla; (b) pressure applied in the two surfaces of the of central incisors (NMP); (c) pressure applied in the surfaces of the CMG model; (d) pressure applied in the surfaces of the FMG and HMG models.

3. Results

Simulations of all models completed all-time steps. Hence, the final load step, corresponding to a 1.5 N total load, was the basis for comparisons among models. These comparisons were based on the qualitative interpretation of the band plots and quantitative analysis of the displacement, strain, stress, and strain energy of different element groups at the same load step.

3.1. Overall Displacements

The displacements over each axes direction and its magnitude were analyzed. A symmetrical distribution was obtained in each group of elements for each numerical model. In all models, the displacement value reaches its maximum in the loaded zone. However, there is a notable quantitative difference in values from one numerical model to the other.

3.1.1. Mouthguard Protections

Mouthguards showed higher displacement in the y-axis coincident with the sagittal plane's vertical direction, representing a vertical sliding movement of the mouthguard. Nevertheless, because the mandible contact did not limit this displacement, it is not realistic. Hence, it was the displacement in the x-axes that was analyzed in more detail. This direction coincides with the load direction, and it is expected that the mouthguard protection has a more relevant effect than in any other direction. The histogram of the distribution of nodal displacements in the x-axis is displayed in Figure 4.

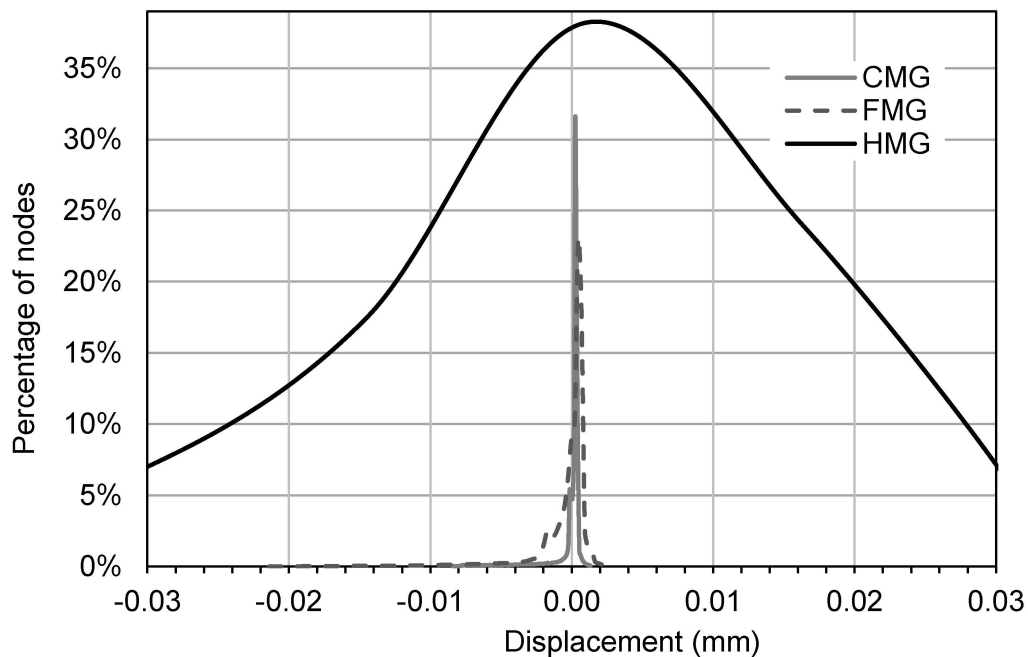


Figure 4. Histograms of the distributions found for the movement antero-posterior, i.e., in the direction of the x-axis, in all mouthguards.

The results presented in Figure 4 for the hollow mouthguard protection are listed only in the range of $-0.03/0.03$ mms, but, as it is possible to see in Table 4, the range is of $-1.48/0.06$ mms; however, if this range were used instead, it would not allow good visualization of behaviors.

Table 4. Mean and range of displacements for the different mouthguard protections.

| Displacement | Model | Mean \pm SD (μm) | Min/Max (μm) |
|--------------|-------|---------------------------------|---------------------------|
| x-axes | CMG | -0.20 ± 1.26 | $-8.33/1.212$ |
| | FMG | -0.65 ± 2.39 | $-21.39/2.58$ |
| | HMG | -20.105 ± 85.42 | $-1480.7/62.63$ |
| y-axes | CMG | -0.76 ± 1.12 | $-2.33/5.71$ |
| | FMG | -1.73 ± 1.97 | $-4.83/10.46$ |
| | HMG | -50.14 ± 68.19 | $-815.17/48.45$ |
| z-axes | CMG | -0.144 ± 0.85 | $-5.29/3.09$ |
| | FMG | -0.06 ± 2.11 | $-10.08/9.35$ |
| | HMG | -2.74 ± 31.96 | $-208.70/89.20$ |
| Magnitude | CMG | 1.62 ± 1.26 | $0.18/9.94$ |
| | FMG | 3.48 ± 2.31 | $0.65/21.61$ |
| | HMG | 69.21 ± 105.38 | $3.69/1688.50$ |

3.1.2. Mouth Components

Table 5 shows the main information of the teeth displacements regarding the mean and range values. The higher displacements appear in the two central incisors in all models, i.e., in the loading region. Moreover, the distribution pattern of the displacement field in all three directions was similar between models. Figure 5 represents the pattern distribution of the magnitude of displacement in all models.

Table 5. Mean and range of displacements of the teeth in the different models.

| Displacement | Model | Mean ± SD (µm) | Min/Max (µm) |
|--------------|-------|-----------------|--------------|
| x-axes | NMG | -0.023 ± 0.047 | -0.558/0.060 |
| | CMG | -0.019 ± 0.0388 | -0.441/0.061 |
| | FMG | -0.018 ± 0.034 | -0.419/0.049 |
| | HMG | -0.008 ± 0.015 | -0.066/0.036 |
| y-axes | NMG | -0.116 ± 0.107 | -0.747/0.004 |
| | CMG | -0.110 ± 0.099 | -0.679/0.004 |
| | FMG | -0.096 ± 0.088 | -0.608/0.003 |
| | HMG | -0.008 ± 0.015 | -0.175/0.006 |
| z-axes | NMG | 0.005 ± 0.022 | -0.080/0.155 |
| | CMG | -0.012 ± 0.023 | -0.134/0.026 |
| | FMG | -0.003 ± 0.019 | -0.071/0.036 |
| | HMG | -0.003 ± 0.010 | -0.045/0.017 |
| Magnitude | NMG | 0.125 ± 0.112 | 0.0004/0.931 |
| | CMG | 0.118 ± 0.101 | 0.0004/0.799 |
| | FMG | 0.103 ± 0.089 | 0.0003/0.726 |
| | HMG | 0.072 ± 0.045 | 0.0003/0.178 |

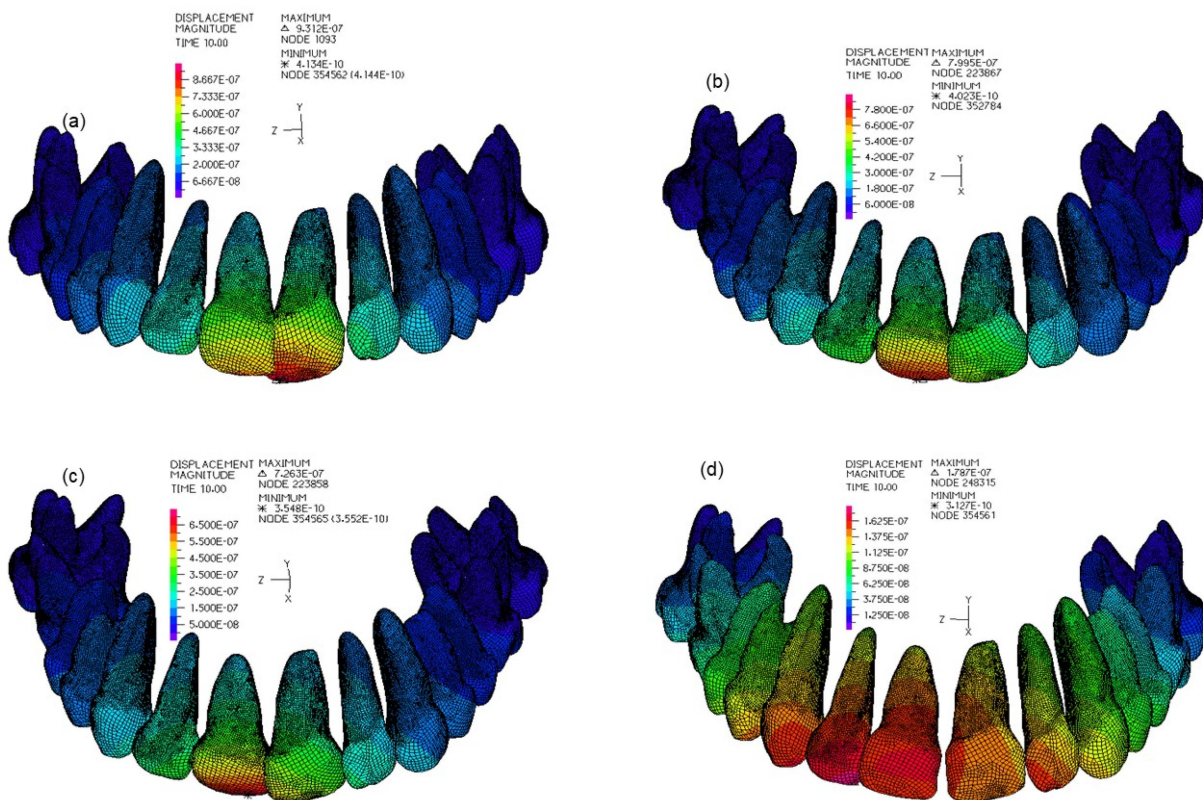


Figure 5. Pattern distribution of the magnitude of displacement field: (a) in the NMG model; (b) in the CMG model; (c) in the FMG model; (d) in the HMG model.

Figure 6 shows the numerical variation of the average teeth displacement with the load intensity. Although the dentition of the four models presented similar behavior, i.e., the average displacement value increases with the increase of the applied force, the HMG model is the one that stands out for giving lower values, and the NMG model for presenting higher values.

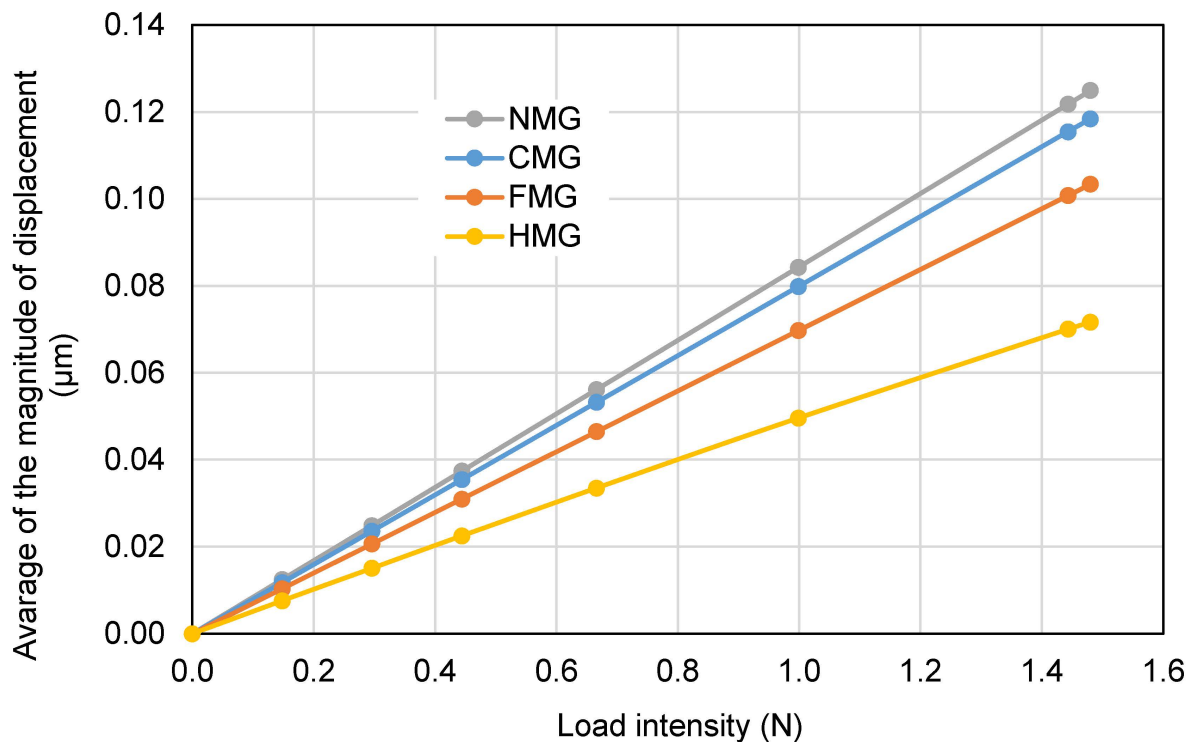


Figure 6. Numerical variation of the average magnitude of displacement with the load intensity.

Table 6 shows the average and the range values of displacements in the maxilla and in the soft tissue. Again, the results show that the HMG model is the one that stands out for presenting lower values of the magnitude of displacement in the maxilla bone and higher values in the soft tissue. Figure 7 shows the main differences among the distributions of the displacement magnitude in the soft tissue of all models.

Table 6. Mean and range of displacements over the maxilla bone and the soft tissue.

| Displ. | Model | Maxilla Bone (nm) | | Soft Tissue (nm) | |
|-----------|-------|----------------------|--------------------|-------------------------|-----------------------|
| | | Mean \pm SD | Min/Max | Mean \pm SD | Min/Max |
| x-axes | NMG | -1.542 ± 22.151 | $-126.550/159.470$ | -70.270 ± 212.100 | $-1028.910/1319.900$ |
| | CMG | -1.167 ± 21.282 | $-119.730/152.430$ | -243.570 ± 651.280 | $-9516.100/1979.200$ |
| | FMG | -1.923 ± 18.284 | $-110.970/135.630$ | -422.500 ± 1244.000 | $-12,991.00/1187.500$ |
| | HMG | -0.321 ± 12.988 | $-29.358/79.253$ | -443.180 ± 1781.600 | $-29,694.00/9175.000$ |
| y-axes | NMG | -80.685 ± 71.675 | $-359.730/29.878$ | -147.070 ± 193.290 | $-1050.300/903.380$ |
| | CMG | -78.313 ± 68.102 | $-350.640/31.506$ | -137.380 ± 476.280 | $-4036.400/5212.50$ |
| | FMG | -67.587 ± 598.20 | $-318.350/27.140$ | -209.450 ± 927.590 | $-10,059.00/7843.20$ |
| | HMG | -52.562 ± 31.950 | $-158.310/17.040$ | -208.770 ± 1140.00 | $-16,598.00/12038.0$ |
| z-axes | NMG | 7.0434 ± 13.995 | $-34.142/55.197$ | 0.08645 ± 182.090 | $-989.000/917.2100$ |
| | CMG | -2.9876 ± 15.787 | $-54.718/37.282$ | -75.214 ± 326.720 | $-5200.900/1843.900$ |
| | FMG | 2.1887 ± 13.639 | $-41.207/35.577$ | 31.325 ± 908.980 | $-7921.800/8249.700$ |
| | HMG | 0.98216 ± 7.3187 | $-21.353/23.638$ | -60.009 ± 902.660 | $-13,011.000/8043.30$ |
| Magnitude | NMG | 85.533 ± 71.203 | $0/365.480$ | 283.880 ± 247.95 | $2.937/1774.600$ |
| | CMG | 83.142 ± 67.606 | $0/356.070$ | 473.290 ± 785.88 | $3.727/11,007.00$ |
| | FMG | 71.876 ± 59.245 | $0/323.310$ | 733.939 ± 1708.4 | $1.837/16,052.90$ |
| | HMG | 55.136 ± 38.456 | $0/158.760$ | 817.070 ± 2205.5 | $5.178/29930.00$ |

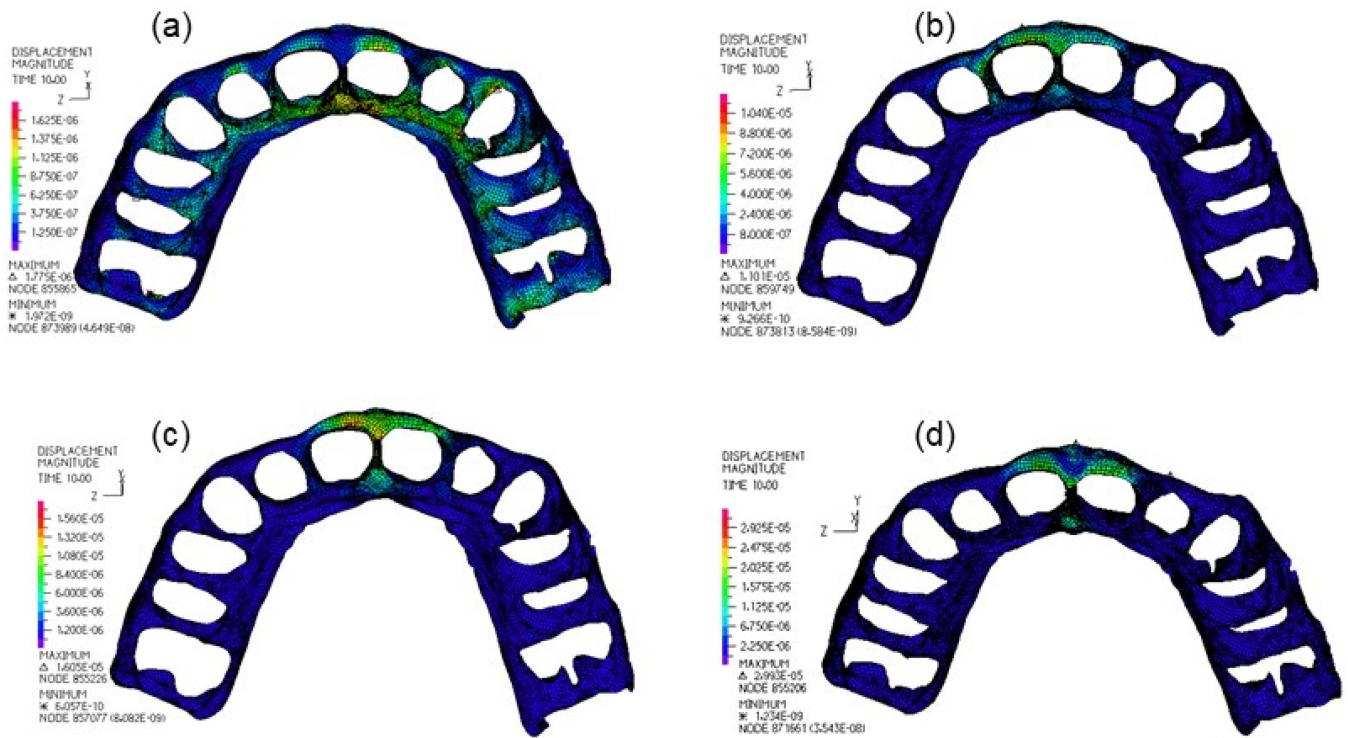


Figure 7. Distribution of the magnitude displacements in the soft tissue: (a) for the NMG model; (b) for the CMG model; (c) for the FMG model; (d) for the HMG modal.

3.2. Overall Strains and Stresses

Stresses and stretches over the mouthguard of each numerical model were evaluated. Regarding the first main stretch, the greater its value, the greater the elongation of the material will be. On the contrary, the smaller the third stretch value, the greater will be the compression level of the material. For the finite elements of bone and teeth, only the analysis of von Mises stresses was performed.

3.2.1. Mouthguard Protections

The material in the loading zones presented higher elongation and higher compression than around this region in all mouthguards, as it is possible to visualize in Figure 8. But because the range color values are different between the mouthguard protections presented in Figure 8, the main differences are not easily visible. Therefore, Table 7 is used to show the quantitative differences between models.

Table 7. Mean and range of stretches over the mouthguard protections.

| Model | First Principal Stretches | | Third Principal Stretches | |
|-------|---------------------------|-------------|---------------------------|---------------|
| | Mean ± SD | Min/Max | Mean ± SD | Min/Max |
| CMG | 1.000 ± 0.0002 | 1.000/1.002 | 0.9999 ± 0.0002 | 0.9974/1.000 |
| FMG | 1.000 ± 0.0002 | 1.000/1.002 | 0.9999 ± 0.0003 | 0.9972/1.000 |
| HMG | 1.002 ± 0.0058 | 1.000/2.549 | 0.9983 ± 0.0038 | 0.3852/0.9999 |

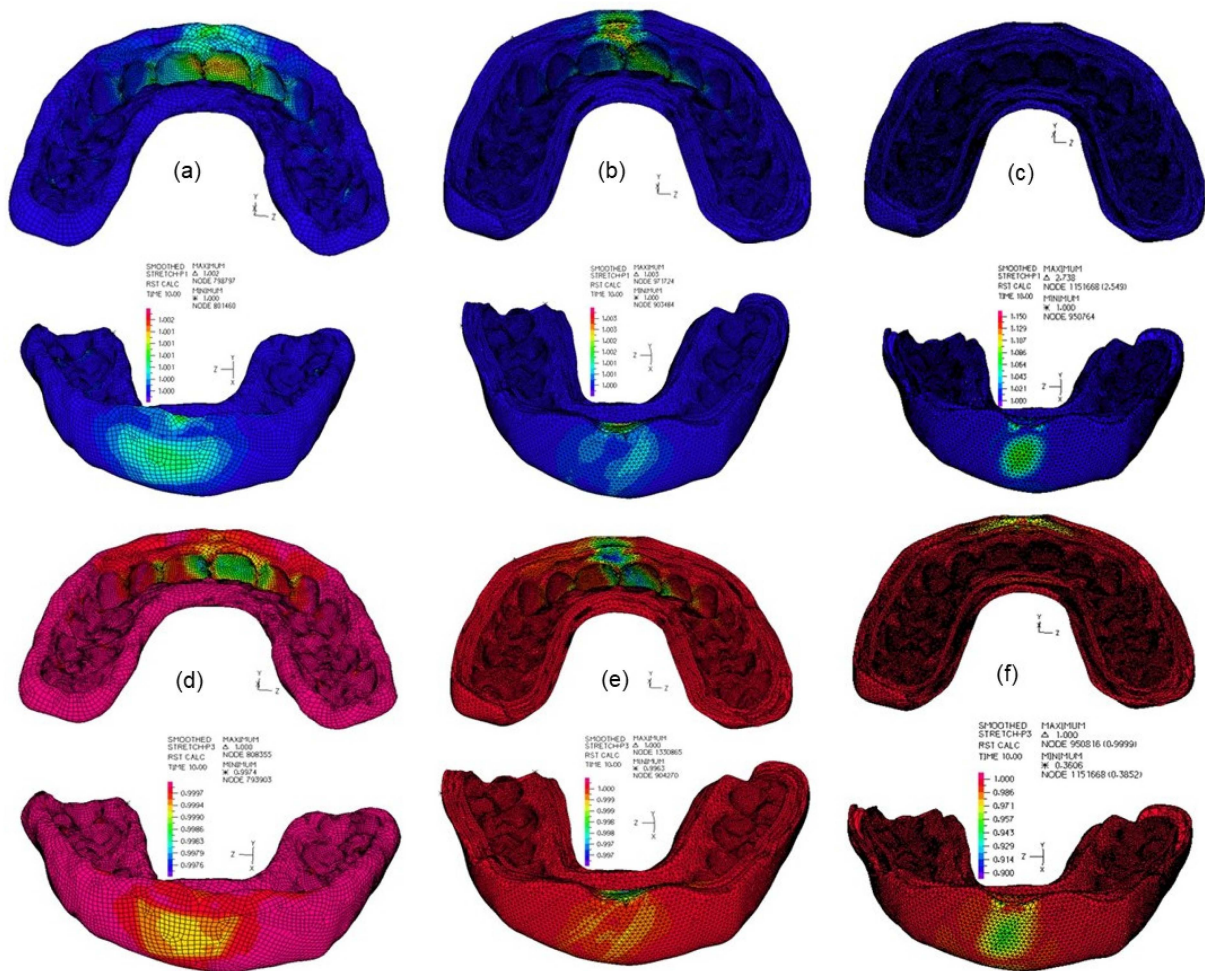


Figure 8. First principal stretches: (a) in the CMG; (b) in the FMG; (c) in the FMG. Third principal stretches: (d) in the CMG; (e) in the FMG; (f) in the HMG.

The results show that the HMG model presents higher values of first principal stretches and lower values of third principal stretches, i.e., it shows greater elongation and compression due to the flexibility of its outer layer, compared to FMG and CMG.

The distribution patterns of the von Mises stress in the mouthguard protections are relatively similar, i.e., the higher values appear in the loading region for all mouthguard protections, but the HMG model shows a higher concentration of values in the loading region than in any other design. The average difference of the von Mises stresses between models is presented in Table 8.

Table 8. Mean and range of stretches over the mouthguard protections.

| Model | Von Mises (KPa) | |
|-------|-----------------|-------------|
| | Mean ± SD | Min/Max |
| CMG | 0.861 ± 2.04 | 0.007/20.8 |
| FMG | 1.05 ± 2.54 | 0.004/32.2 |
| HMG | 3.29 ± 89.2 | 0.008/11392 |

3.2.2. Mouth Components

The von Mises stresses over the teeth were plotted for all the models, and the patterns of the stress distributions were similar; critical regions appears in the roots of the central incisors. The mean and range of von Mises stresses in the teeth are presented in Table 9 for all models. Figure 9 emphasis the stress distribution pattern in the case of no mouthguard being worn.

Table 9. Mean and range of von Mises stresses in the teeth and the maxilla bone.

| Model | Von Mises (KPa) | | | |
|-------|-----------------|---------------|-----------------|----------|
| | Teeth | | Maxilla Bone | |
| | Mean ± SD | Min/Max | Mean ± SD | Min/Max |
| NMG | 16.14 ± 22.070 | 0.031/415.900 | 16.851 ± 18.161 | 0/672.12 |
| CMG | 13.79 ± 16.370 | 0.014/372.900 | 15.188 ± 14.066 | 0/578.91 |
| FMG | 12.50 ± 15.060 | 0.033/316.800 | 13.642 ± 12.762 | 0/460.35 |
| HMG | 6.087 ± 4.146 | 0.013/62.840 | 7.4123 ± 5.3319 | 0/226.98 |

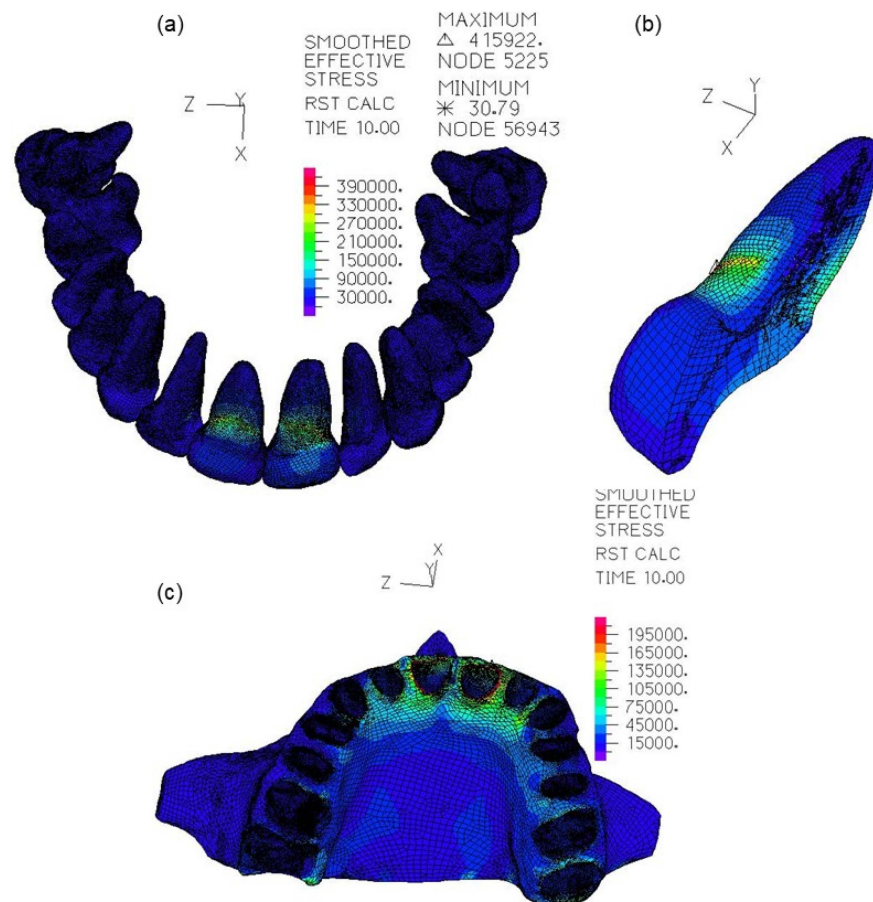


Figure 9. Von Mises stress distribution for the NMP model: (a) in the teeth; (b) central incisor cut; (c) maxilla bone.

For the bone tissue, the stress concentration area was at the crestal level of the alveolar bone in the buccal side, regardless of the design or material used in the mouthguard. Moreover, as shown in Figure 9c, in the case of no mouthguard protection being worn, the von Mises stress distribution over the maxilla bone also showed a similar pattern.

The soft tissue in the loading zones also presented higher elongation and higher compression. Table 10 is used to present the average and the range of first and third principal stretches in the soft tissue for all models.

Table 10. Mean and range of stretches over the soft tissue.

| Model | First Principal Stretches | | Third Principal Stretches | |
|-------|---------------------------|----------------|---------------------------|----------------|
| | Mean \pm SD | Min/Max | Mean \pm SD | Min/Max |
| NMP | 1.0001 \pm 0.00009 | 0.99996/1.0060 | 0.99992 \pm 0.0000804 | 0.99453/1.0000 |
| CMP | 1.0002 \pm 0.00054 | 0.99980/1.0150 | 0.9977 \pm 0.00066099 | 0.96075/1.0016 |
| FMP | 1.0003 \pm 0.00088 | 0.99988/1.0222 | 0.99964 \pm 0.0009374 | 0.98476/1.0000 |
| HMP | 1.0005 \pm 0.00139 | 0.99996/1.0680 | 0.99950 \pm 0.0015838 | 0.90862/1.0000 |

The lowest value of mean von Mises stresses in the soft tissue was 0.047209 ± 0.045130 KPa, and it was detected in the model without mouthguard protection. On the contrary, the highest mean von Mises stress value was presented in the HMG model, showing a mean of 0.26127 ± 0.79498 KPa. In the CMG and FMG models, the mean value of von Mises stress was of 0.12466 ± 0.30624 KPa and $0.19221 \pm 0.481.25$ KPa, respectively.

4. Discussion

This study aimed to investigate the influence of mouthguard wearing in reducing the stress magnitude on the involved structures during a dental trauma, namely in the maxilla central incisors. The present study also focused on evaluating the influence of the material and design of the MG in the level of von Mises stresses through mouth components. Four models were compared, one featuring a human maxilla without mouth protection and three with different mouthguard protections. Finite element analysis studies regarding the influence of wearing a mouthguard during an impact in the orofacial region have already been published [13,24–27], but the work now presented is, to our knowledge, the first nonlinear analysis offering a three-dimensional comparison of an air-filled mouthguard. Moreover, it is also the first one accounting for the soft tissue surrounding maxilla bone and teeth.

The results show that the presence of an MG is associated with a decrease in the stress magnitudes of teeth and maxilla bone but an increase in the soft tissue von Mises stresses. Though the simulated mouthguards had 4 mm of thickness, because some relevant studies described this parameter to be in the range of 3 to 4 mm as an ideal condition [8,11–13,24,28], thinner mouthguards may have different results. Another design parameter that can condition the level of mouth protection is the mouthguard material. In fact, the different mouthguard materials resulted in different patterns of mouthguard displacements. In Figure 4, it is possible to observe the main differences of the antero-posterior movement between all mouthguards, while in Table 4, it is possible to quantify the main differences of the average displacements. Comparison of the magnitude displacement between CMG and FMG reveals that the last model presented a higher mean value, which could be due to the presence of the inner layer of EVA foam being less rigid than EVA. Comparing CMG with HMG, it is also possible to detect an increase in the average displacement values in the presence of an air layer. This layer will allow the HMG's outer layer a superior flexibility of movement, thus allowing the increase of energy dissipation between layers. Although HMG has higher average values of magnitude and of x-displacements, in the histogram of the distributions found for the anteroposterior movement, it is also the HMG model associated with a higher percentage of nodal points that does not show displacement in the x-axis. This behavior can be explained by the nodal points associated with the layer in contact with the teeth, whose displacement is smaller than in the other models; see, for example, the teeth displacements presented in Figure 5d or the results of Figure 6. A similar effect was reported by Westerman et al. [14], wherein the maximum transmitted force through the air inclusion in the EVA material was reduced by 32%. Later, Takeda et al. [15] also reported that space between the tooth surface and the mouthguard material showed a relatively high shock-absorbing tooth distortion.

The distributions of the magnitude of displacement in the teeth showed a similar pattern, as presented in Figure 5, but the average values of teeth displacements showed

values that were as large as were small the average displacements of their respective MG numerical models. The model with the higher displacements was that without mouthguard protection. Hence, compared to this one, in the CMG model the displacement was 5.6% lower, in the FMG model it was 17.6% lower, and in the HMG model it was 42.4% lower, as can be verified in Table 5 and Figure 6. The average values of the magnitude of bone displacement were about 2.8%, 15.9%, and 35.5% lower in the CMG, FMG, and HMG models, respectively, to that of the NMG model. Nevertheless, the average values of the magnitude of tissue displacement increased by about 66.7%, 158.5%, and 187.8% in the CMG, FMG, and HMG models, respectively, to that of the NMG model. Hence, these results, and those presented in Table 10, seem to indicate that improving the mouthguard flexibility can be responsible for the increase of soft tissue injuries. Nevertheless, when dental injuries are restricted to the soft tissues, such as lacerations, abrasions, and contusions, they create wounds that usually heal without major complications [29].

The stresses and stretches over the mouthguard reveal its ability to shock absorption, which depends in the material shock absorption ability. The EVA and the EVA foam materials show good energy absorption capabilities [1,8,9,14,28] and, therefore, all the three mouthguards are well positioned relatively to this parameter. Nevertheless, it was the HMG model that presented higher values of first principal stretches and lower values of third principal stretches, i.e., it shows greater elongation and compression, due to the flexibility of its outer layer, compared to FMG and CMG models. but it was also the HMG model that showed higher stress in the loading region. Hence, these results show that air inclusion in EVA mouthguard materials may change the impact characteristics and performance of this polymer [14,15].

The von Mises stresses over teeth showed critical regions in the roots of central incisors in all models, but the higher values appear in the NMG model. The results of Table 9 show that, compared to NMG, the wearing of a compact EVA mouthguard (CMG) allowed the reduction of the von Mises stresses in 14.5%, whereas wearing the EVA/EVA Foam/EVA mouthguard (FMG) reduces the von Mises stresses in 22.6% and, finally, wearing an EVA/hollow/EVA mouthguard (HMG) reduces the von Mises stresses in 62.5%. In any of the cases, the maximum values of effective stress detected do not exceed the elasticity limit of the tooth and, therefore, it is concluded that there was no fracture of the teeth. For the bone tissue, the stress concentration area was at the crestal level of the alveolar bone in the buccal side, regardless of the design or material used in the mouthguard. Some of the published finite element studies do show a different critical area in the maxilla bone [16]. This behavior can be justified with the presence or not of the periodontal ligament (PDL). In fact, as shown by Jang et al. [30] and by Borges et al. [26], the deterioration of the PDL mechanical characteristics might alter the biomechanical response of the tooth. Nevertheless, the present study corroborated with all of these previous statements, showing a stress magnitude decrease associated with the wearing of MGs. Moreover, as showed by Borges et al., wearing an MG in a deteriorated PDL reduces the stress magnitude at a smaller level than in the sound PDL model. Hence, if the PDL were included in all geometrical and numerical models [18], it would be expected that those results related to MG use would be amplified.

Some limitations of this study are related to the geometrical and mechanical properties of the maxilla bone and of the teeth. As is well known, maxilla bone has variability in cortical and cancellous mechanical properties [31], and the tooth structure is more complex [32,33] than the one used in the present work. Nevertheless, because this is a comparative study and the realistic mechanical properties of all components will remain in the linear elasticity range, it is expected that these simplification assumptions will affect all models similarly. Hence, the comparison results should remain almost unchanged. There are other physical factors not accounted for in this study, such as the presence of the mandible to contact with the maxilla, which can change the mouthguard movement during the loading, or the presence of an impactor object, which can change the intensity and loading area.

5. Conclusions

Within the limitations of the present study and those of finite element analysis, it is possible to conclude that all the tested mouthguards show different behavior to static loading, and it is possible to draw the following conclusions:

- Wearing any of the analyzed mouthguards reduces the risk of injury to teeth and bone, as they reduce the displacement, strain, and stress of these structures;
- Soft damping systems, such as EVA foam, included in the FMG model, show greater deformation, increasing the contact time between objects and, therefore, promoting greater energy dissipation in a larger area, thus reducing the damage to a specific point;
- The implementation of a space layer, as was the case in the HMG model, allows greater displacement and deformation of the external layers of the mouthguard, allowing greater energy absorption and thus greater protection of the anatomic structures, namely the root dentin and the bone tissue;
- Nevertheless, the results also indicate that improving the mouthguard flexibility can be responsible for the increase of soft tissue injuries.

Author Contributions: Conceptualization, A.M.; methodology, M.A.N.; software, I.J.G.; validation, A.M., A.M.A., P.N.B.R. and M.A.N.; formal analysis, I.J.G., A.M. and M.A.N.; writing—original draft preparation, M.A.N.; writing—review and editing, A.M., A.M.A. and P.N.B.R.; All authors have read and agreed to the published version of the manuscript.

Funding: This research is sponsored by national funds through FCT—Fundação para a Ciência e a Tecnologia, under the project UIDB/00285/2020.

Institutional Review Board Statement: Not applicable.

Informed Consent Statement: Not applicable.

Data Availability Statement: Not applicable.

Acknowledgments: In this section, you can acknowledge any support given which is not covered by the author contribution or funding sections. This may include administrative and technical support, or donations in kind (e.g., materials used for experiments).

Conflicts of Interest: The authors declare no conflict of interest.

References

1. Moreira, M.; Ramos, J.C.; Messias, A.; Neto, M.A.; Amaro, A.P.; Reis, P.N. Impact response of different materials for sports mouthguards. *Frat. ed Integrità Strutt.* **2021**, *15*, 63–69. [[CrossRef](#)]
2. Wang, R.; Habib, E.; Zhu, X.X. Evaluation of the filler packing structures in dental resin composites: From theory to practice. *Dent. Mater.* **2018**, *34*, 1014–1023. [[CrossRef](#)]
3. Khosravani, M.R. Mechanical behavior of restorative dental composites under various loading conditions. *J. Mech. Behav. Biomed. Mater.* **2019**, *93*, 151–157. [[CrossRef](#)]
4. Knapik, J.J.; Marshall, S.W.; Lee, R.B.; Darakjy, S.S.; Jones, S.B.; Mitchener, T.A.; Delacruz, G.G.; Jones, B.H. Mouthguards in sport: Activities history, physical properties and injury prevention effectiveness. *Sport. Med.* **2007**, *37*, 117–144. [[CrossRef](#)] [[PubMed](#)]
5. Green, J.I. The Role of Mouthguards in Preventing and Reducing Sports-related Trauma. *Prim. Dent. J.* **2017**, *6*, 27–34. [[CrossRef](#)] [[PubMed](#)]
6. Lauridsen, E.; Andreassen, J.O.; Bouaziz, O.; Andersson, L. Risk of ankylosis of 400 avulsed and replanted human teeth in relation to length of dry storage: A re-evaluation of a long-term clinical study. *Dent. Traumatol.* **2020**, *36*, 108–116. [[CrossRef](#)]
7. Takeda, T.; Ishigami, K.; Shintaro, K.; Nakajima, K.; Shimada, A.; Regner, C.W. The influence of impact object characteristics on impact force and force absorption by mouthguard material. *Dent. Traumatol.* **2004**, *20*, 12–20. [[CrossRef](#)]
8. Carvalho, V.; Soares, P.; Verissimo, C.; Pessoa, R.; Versluis, A.; Soares, C. Mouthguard Biomechanics for Protecting Dental Implants from Impact: Experimental and Finite Element Impact Analysis. *Int. J. Oral Maxillofac. Implants* **2018**, *33*, 335–343. [[CrossRef](#)]
9. Bridgman, H.; Kwong, M.T.; Bergmann, J.H.M. Mechanical Safety of Embedded Electronics for In-body Wearables: A Smart Mouthguard Study. *Ann. Biomed. Eng.* **2019**, *47*, 1725–1737. [[CrossRef](#)]
10. Westerman, B.; Stringfellow, P.M.; Eccleston, J.A. The effect on energy absorption of hard inserts in laminated EVA mouthguards. *Aust. Dent. J.* **2000**, *45*, 21–23. [[CrossRef](#)]
11. Westerman, B.; Stringfellow, P.M.; Eccleston, J.A. EVA mouthguards: How thick should they be? *Dent. Traumatol.* **2002**, *18*, 24–27. [[CrossRef](#)] [[PubMed](#)]

12. Cummins, N.K.; Spears, I.R. The effect of mouthguard design on stresses in the tooth-bone complex. *Med. Sci. Sports Exerc.* **2002**, *34*, 942–947. [[CrossRef](#)]
13. Verissimo, C.; Costa, P.V.M.; Santos-Filho, P.C.F.; Tantbirojn, D.; Versluis, A.; Soares, C.J. Custom-Fitted EVA Mouthguards: What is the ideal thickness? A dynamic finite element impact study. *Dent. Traumatol.* **2016**, *32*, 95–102. [[CrossRef](#)]
14. Westerman, B.; Stringfellow, P.M.; Eccleston, J.A. Beneficial effects of air inclusions on the performance of ethylene vinyl acetate (EVA) mouthguard material. *Br. J. Sports Med.* **2002**, *36*, 51–53. [[CrossRef](#)]
15. Takeda, T.; Ishigami, K.; Handa, J.; Naitoh, K.; Kurokawa, K.; Shibusawa, M.; Nakajima, K.; Kawamura, S. Does hard insertion and space improve shock absorption ability of mouthguard? *Dent. Traumatol.* **2006**, *22*, 77–82. [[CrossRef](#)]
16. Tribst, P.J.M.; Dal Piva, A.M.D.O.; Ausiello, P.; De Benedictis, A.; Bottino, M.A.; Luiz, A.; Borges, S. Biomechanical Analysis of a Custom-Made Mouthguard Reinforced With Different Elastic Modulus Laminates During a Simulated Maxillofacial Trauma. *Craniofacial Trauma Reconstr.* **2021**, *14*, 254–260. [[CrossRef](#)] [[PubMed](#)]
17. Neto, M.A.; Amaro, A.; Luis, R.; Cirne, J.; Leal, R. *Engineering Computation of Structures: The Finite Element Method*; Springer: Aargau, Switzerland, 2015; ISBN 9783319177106/9783319177090.
18. Messias, A.; Neto, M.A.; Amaro, A.M.; Lopes, V.M.; Nicolau, P. Mechanical evaluation of implant-assisted removable partial dentures in kennedy class i patients: Finite element design considerations. *Appl. Sci.* **2021**, *11*, 659. [[CrossRef](#)]
19. Schwartz-Dabney, C.L.; Dechow, P.C. Edentulation alters material properties of cortical bone in the human mandible. *J. Dent. Res.* **2002**, *81*, 613–617. [[CrossRef](#)] [[PubMed](#)]
20. Schwartz-Dabney, C.L.; Dechow, P.C. Variations in cortical material properties throughout the human dentate mandible. *Am. J. Phys. Anthropol.* **2003**, *120*, 252–277. [[CrossRef](#)]
21. Odin, G.; Savoldelli, C.; Bouchard, P.O.; Tillier, Y. Determination of Young's modulus of mandibular bone using inverse analysis. *Med. Eng. Phys.* **2010**, *32*, 630–637. [[CrossRef](#)]
22. Messias, A.; Neto, M.A.; Amaro, A.M.; Nicolau, P.; Roseiro, L.M. Effect of round curvature of anterior implant-supported zirconia frameworks: Finite element analysis and in vitro study using digital image correlation. *Comput. Methods Biomech. Biomed. Engin.* **2017**, *20*, 1236–1248. [[CrossRef](#)]
23. Zhang, Y.R.; Du, W.; Zhou, X.D.; Yu, H.Y. Review of research on the mechanical properties of the human tooth. *Int. J. Oral Sci.* **2014**, *6*, 61–69. [[CrossRef](#)] [[PubMed](#)]
24. Gialain, I.O.; Coto, N.P.; Driemeier, L.; Noritomi, P.Y.; Dias, R.B.E. A three-dimensional finite element analysis of the sports mouthguard. *Dent. Traumatol.* **2016**, *32*, 409–415. [[CrossRef](#)] [[PubMed](#)]
25. Paulo, J.; Tribst, M.; Dal Piva, A.M.D.O.; Luiz, A.; Borges, S.; Bottino, M.A. Simulation of mouthguard use in preventing dental injuries caused by different impacts in sports activities. *Sport Sci. Health* **2019**, *15*, 85–90.
26. Borges, A.L.S.; Dal Piva, A.M.D.O.; Concílio, L.R.D.S.; Paes-Junior, T.J.D.A.; Tribst, J.P.M. Mouthguard use effect on the biomechanical response of an ankylosed maxillary central incisor during a traumatic impact: A 3-dimensional finite element analysis. *Life* **2020**, *10*, 294. [[CrossRef](#)] [[PubMed](#)]
27. Tribst, J.P.M.; Dal Piva, A.M.D.O.; Bottino, M.A.; Kleverlaan, C.J.; Koolstra, J.H. Mouthguard use and TMJ injury prevention with different occlusions: A three-dimensional finite element analysis. *Dent. Traumatol.* **2020**, *36*, 662–669. [[CrossRef](#)] [[PubMed](#)]
28. Ozawa, T.; Takeda, T.; Ishigami, K.; Narimatsu, K.; Hasegawa, K.; Nakajima, K.; Noh, K. Shock absorption ability of mouthguard against forceful, traumatic mandibular closure. *Dent. Traumatol.* **2014**, *30*, 204–210. [[CrossRef](#)] [[PubMed](#)]
29. Mordini, L.; Lee, P.; Lazaro, R.; Biagi, R.; Giannetti, L. Sport and Dental Traumatology: Surgical Solutions and Prevention. *Dent. J.* **2021**, *9*, 33. [[CrossRef](#)]
30. Jang, Y.; Hong, H.T.; Chun, H.J.; Roh, B.D. Influence of Dentoalveolar Ankylosis on the Biomechanical Response of a Single-rooted Tooth and Surrounding Alveolar Bone: A 3-dimensional Finite Element Analysis. *J. Endod.* **2016**, *42*, 1687–1692. [[CrossRef](#)]
31. Peterson, J.; Wang, Q.; Dechow, P.C. Material properties of the dentate maxilla. *Anat. Rec.—Part A Discov. Mol. Cell. Evol. Biol.* **2006**, *288*, 962–972. [[CrossRef](#)]
32. Jiang, Q.; Huang, Y.; Tu, X.R.; Li, Z.; He, Y.; Yang, X. Biomechanical Properties of First Maxillary Molars with Different Endodontic Cavities: A Finite Element Analysis. *J. Endod.* **2018**, *44*, 1283–1288. [[CrossRef](#)]
33. Neto, M.A.; Roseiro, L.; Messias, A.; Falacho, R.I.; Palma, P.J.; Amaro, A.M. Influence of cavity geometry on the fracture strength of dental restorations: Finite element study. *Appl. Sci.* **2021**, *11*, 4218. [[CrossRef](#)]